Master's Thesis

Differential Power Processing Converter Design for a Photovoltaic-Powered Charging Bag

Hyun-Ji Lee

Department of Electrical Engineering

Graduate School of UNIST

2017

Differential Power Processing Converter Design for a Photovoltaic-Powered Charging Bag

Hyun-Ji Lee

Department of Electrical Engineering

Graduate School of UNIST

Differential Power Processing Converter Design for a Photovoltaic-Powered Charging Bag

A thesis/dissertation
submitted to the Graduate School of UNIST
in partial fulfillment of the
requirements for the degree of
Master of Science

Hyun-Ji Lee

12. 16. 2016
Approved by

_____

Advisor
Katherine Ann Kim

Differential Power Processing Converter Design for a Photovoltaic-Powered Charging Bag

Hyun-Ji Lee

This certifies that the thesis/dissertation of Hyun-Ji Lee is approved.

12. 16. 2016

signature

_____

Advisor: Katherine Ann Kim

signature

_____

typed name: Jeehoon Jung

signature

_____

typed name: SeongJin Kim

ABSTRACT

Traditional photovoltaic (PV) systems are stationary PV systems mounted in one location and, generally, receive consistent and even illumination across the PV panels. However, solar photovoltaic (PV) power is also getting widely used in lower-power emerging applications, like wearables or internet of things (IoT) devices. One fundamental challenge of using PV power in wearable applications is that individual PV cells may be pointing in different angles, receiving different light intensities.

Under these uneven illumination, resulting system efficiency depends on the configurations of the PV cells and converters. Through this thesis, the system efficiencies of five configurations are compared with nine realistic test cases. The five configurations are: PV in series with central converter, PV in parallel with central converter, PV with cascaded converters, PV in series with differential power processing (DPP) converters, and PV in parallel with DPP converters. The nine test cases are composed of an ideal case (all PV cells at 1,000 W/m^2) and eight realistic illumination cases based on the weather (sunny or cloudy) and realistic usage scenarios. Based on these cases the system efficiency is calculated for each configuration considering a range of converter efficiencies (70% to 100%). Results show that the parallel DPP configuration shows the highest system efficiency in all cases.

Parallel DPP converters can achieve individual PV control and maximizing output power by processing small fraction of the PV power. There are two types of parallel DPP architectures which are with and without a front-end converter. Two parallel DPP architectures are analyzed and compared for a target 5-W wearable application. Between the two architectures, the DPP system without a front-end converter shows consistently high performance and operates properly over a wider range of lighting conditions.

Therefore, the proper operation, such as maximum power point tracking (MPPT) of PV cells, using parallel DPP converters without the front-end converter is validated through simulation and hardware experiments. The PV-powered wearable prototype is able to charge a portable battery under low-light and partial shading conditions.

CONTENTS

FIGURE LIST

Fig. 20 Experimental waveforms for the DPP system (a) clamped at 5 V and (b) charging a battery.

Fig. 21 DPP converter efficiency with (a) 5-V input voltage 5 V and output voltage of 2 V and (b) output voltage of 0.5 V.

TABLE LIST

I. INTRODUCTION

Nowadays, portable electronic devices are a necessity in daily life. As people use their mobile devices more often, frequent battery charging is needed. For convenient battery charging and less wear on the battery, wearable charging applications have been explored [1-3]. In this thesis, a photovoltaic (PV)-powered charging bag that can charge portable electronic devices through a USB port power interface is being developed, as shown in Fig. 1.

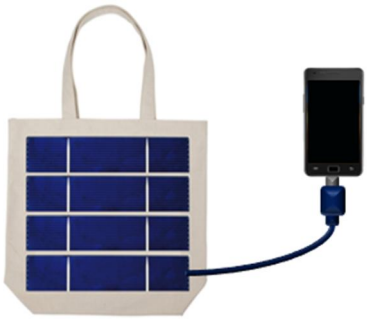

Fig. 1. Prototype of the PV-powered charging

Traditionally, PV systems are typically setup in static places, such as the ground or a roof top. However, due to development of PV cells and power electronics, PV systems are also being used as movable systems, such as electric vehicles, PV clothes, and wearable application [1-6]. One of the challenges in movable PV systems is mismatch in illumination on PV cells. The mismatch in illumination mainly comes from variation of sun light, but can also come from partial shading, manufacturing variance, and degradation [7-8]. Especially in case of PV-powered charging bag, some of the PV cells can become partially shaded by the user's arm, as shown in Fig. 2(a). Also due to the flexible nature of the bag material, each PV cell may point in different directions such that illumination from direct sunlight will not be even for each PV cell, as shown in Fig. 2(b).

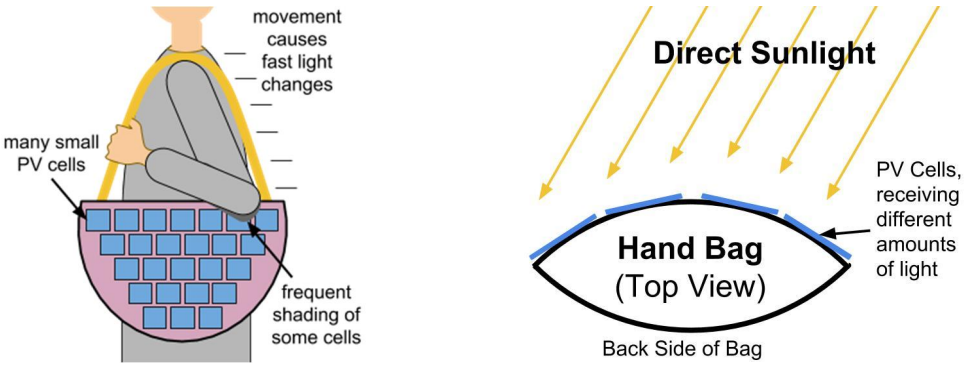

(a) (b)

Fig. 2. Mismatch in illumination due to (a) shading from user's arm, and (b) different incidence angles.

These uneven sunlight conditions result in severe power loss throughout the total PV system, especially in the traditional series configuration [9-10]. To reduce the power loss, various configurations of PV cells and converters have been considered and proposed [17-38]. In most of existing PV systems, PV cells are connected in series or parallel and controlled by a central converter, as shown in Fig. 3(a) and Fig. 3(b). However, in series or parallel configurations, the system output power is greatly reduced when there is a difference among PV cell illumination [11-16]. Because only one converter controls all PV cells, every PV cells should operate with the same current in series configuration or with the same voltage in parallel configuraiton regardless of mismatch in illumination. Therefore, it is hard to make every PV cell operate at own maximum power point (MPP) and the system output power decreases significantly.

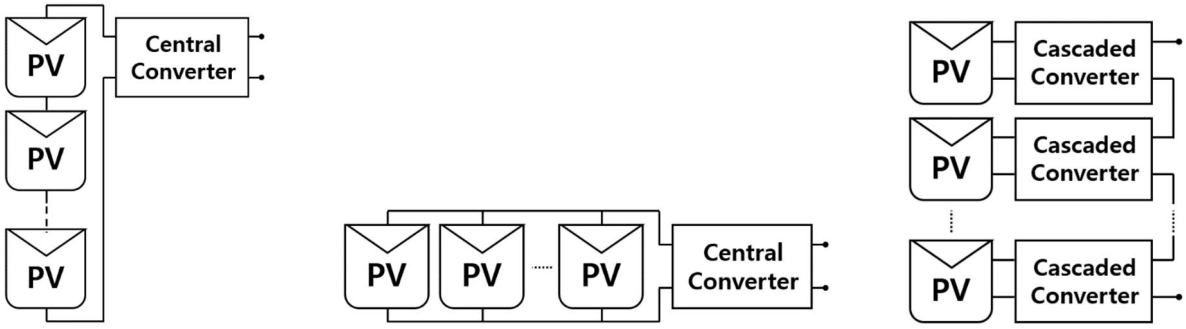

(a) (b) (c)

Fig. 3 Traditional PV and converter configurations (a) series, (b) parallel, and (c) cascaded

Another potential configuration is using cascaded converters [17-19], which allows for each PV cell to be controlled individually, as shown in Fig. 3(c). Because cascaded converters controll each PV cell individually, PV cells can operate at MPP both even and uneven sunlight conditions. A more recently introduced configuration is differential power processing (DPP) converter which also controls PV cells individually, as shown in Fig. 4 [24-38]. Fig. 4(a) shows DPP series configuration and Fig. 4(b) shows DPP parallel configuration. The difference between cascaded converter and DPP converter is that DPP converter processes only partial PV power while cascaded converter processes full PV power. Because DPP converters have much smller power conversion loss in converters, DPP converters can achieve higher efficiency than cascaded converters. For the PV-powered charging bag, parallel DPP converters is applied to get optimal system operation, which is battery charging, under even and uneven sunilght conditions.

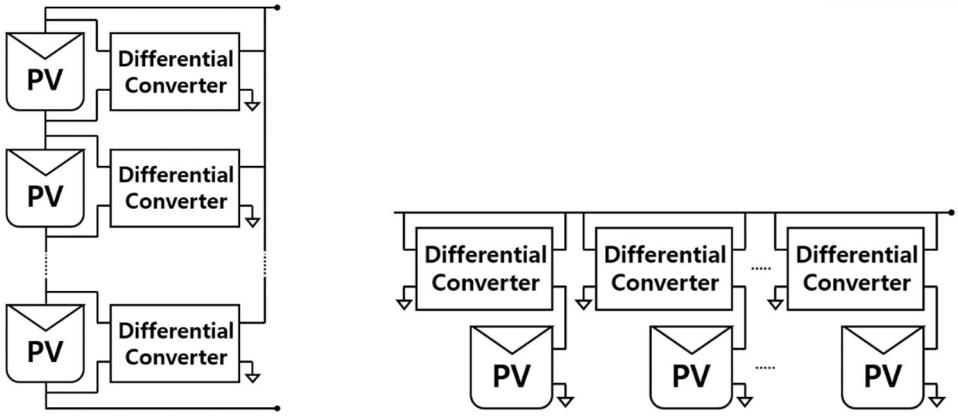

(a) (b)

Fig. 4 DPP converter configurations (a) DPP series, and (b) DPP parallel

In this thesis, the system efficiency of five different configurations in nine different test conditions are calculated and compared in section Ⅱ. In section Ⅲ, the operation of the proposed parallel DPP system is explained. Then, an impedance matching problem between the MPPT control on the PV cell and the battery load is explained and explored in Section Ⅳ. Section Ⅴ shows simulation results of the system and Section Ⅵ and Section Ⅶvalidates the system with hardware experiments results. The findings are summarized and concluded in Section Ⅷ.

II. COMPARISON OF FIVE CONVERTER CONFIGURATIONS

A. PV-powered Charging Bag Modeling and Illumination Test Cases

In order to compare the system output power depending on five different PV and converters configurations, the PV-powered charging bag and PV cells used in the PV bag were modeled in Matlab, as shown in Fig. 5.

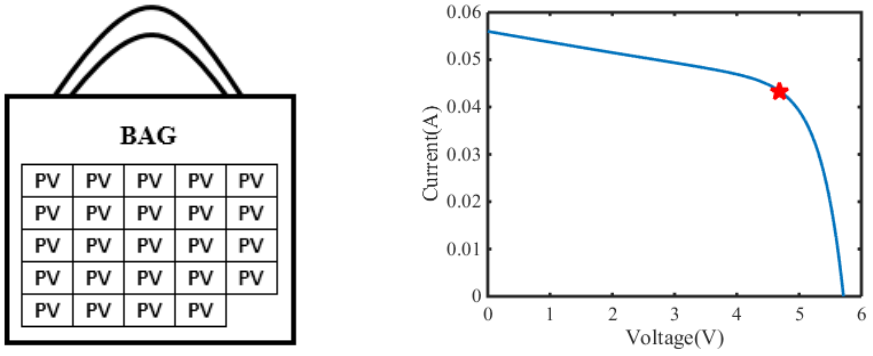

(a) (b)

Fig. 5 (a) PV-powered charging bag with 24 PV cells, and (B) I-V characteristics of a PV cell

Fig. 5(a) shows PV-powered charging bag which is composed of 24 PV cells and Fig. 5(b) shows I-V characteristic of each PV cell used in PV-powered charging bag. When a PV cell receives nominal illumination (1,000 W/m^2), the MPP current is 43 mA and voltage is 4.69 V such that the PV power at MPP is 0.20 W. The PV-powered charging bag consists of 24 PV cells such that the maximum system power is 4.88 W with full illumination. Note that 5 W is a standard power level for charging a mobile device battery. With full illumination, the PV-powered charging bag is able to provide a similar power level with normal USB port for charging mobile devices.

In order to compare various realistic usage cases, nine illumination cases are considered, as outlined in Table I. The first test case is ideal such that all PV cells get 1,000 W/m^2 illumination evenly. The remaining eight cases consist of measured irradiance data taken outdoors under various conditions. The cases are categorized based on weather (sunny or cloudy), whether or not there is partial shading, and whether or not something is in the bag. When the bag is empty, the surface of the bag is relatively flat and the light intensities on each PV cell are fairly uniform. However, when something is in the bag, the incidence angle of sun light on each PV cell is different because of the flexibility of the bag. Therefore, the effective light intensities on each PV cell are also different such that it causes uneven illumination on PV cells.

TABLE □ Nine Illumination Test Cases

Case 01	Ideal cases (All 1,000 W/m^2)		
Case 02	Sunny day	No partial shading	Empty bag
Case 03			Something in the bag
Case 04		Partial shading	Empty bag
Case 05			Something in the bag
Case 06	Cloudy day	No partial shading	Empty bag
Case 07			Something in the bag
Case 08		Partial shading	Empty bag
Case 09			Something in the bag

For each case, the illumination on each of the 24 PV cells was measured outside using an irradiance power meter, as shown in Fig. 6. Fig. 6(a) shows the PV-powered charging bag usage case without partial shading on sunny day and Fig. 6(b) shows the usage case with partial shading on cloudy day. The measured illumination data is provided in Table □. The measured illumination data is used for comparison of five different converter configurations.

(a) (b)

Fig. 6 Realistic usage case of PV-powered charging bag (a) without partial shading, and (B) with partial shading

TABLE Measured Illumination Data of Nine Test Cases *

PV	Case 01	Case 02	Case 03	Case 04	Case 05	Case 06	Case 07	Case 08	Case 09
1	1000	920	1010	1020	1060	490	385	380	300
2	1000	980	1020	995	150	485	390	1	330
3	1000	995	990	1	1	470	405	1	10
4	1000	1000	975	120	750	460	400	470	175
5	1000	990	1005	1015	1115	465	195	415	195
6	1000	1045	1010	1045	1140	460	400	2	275
7	1000	1040	1005	1015	410	465	360	1	1
8	1000	1050	1010	1	1	440	395	445	520
9	1000	1035	1010	100	920	450	230	395	190
10	1000	1020	965	920	920	450	370	5	100
11	1000	1050	980	1040	955	420	360	345	155
12	1000	1065	970	1040	1	380	380	420	495
13	1000	1060	995	1	1	415	375	325	225
14	1000	1065	950	155	970	400	340	10	35
15	1000	1070	835	970	935	380	330	415	140
16	1000	1025	975	1035	935	390	325	410	470
17	1000	1055	930	1020	1	390	330	350	335
18	1000	1060	925	2	1	395	365	5	20
19	1000	1065	915	31	440	405	375	440	275
20	1000	1050	850	1000	654	400	395	420	370
21	1000	1025	880	1020	800	390	330	350	335
22	1000	1085	850	1025	1	395	365	5	20
23	1000	1115	785	5	35	405	375	440	275
24	1000	1100	795	840	265	400	395	420	370

* Illumination unit: W/m^2

B. Power Conversion Loss in Five Different Converter Configurations

The overall system output power is highly affected by the configurations of PV cells and converters. Especially when there is mismatch in illumination, the system output power varies a lot depending on the converter configurations. To get optimal system output power under various realistic usage cases, the following five different converter configurations are considered: series, parallel, cascaded, DPP series, and DPP parallel.

1) Series

In the series configuration, PV cells are connected in series to a central converter which achieves MPPT of total PV system, as shown in Fig. 3(a). Series configuration is the most traditional configuration that is widely used by default. However, because the PV cells are not controlled individually, the series string current is limited by the PV cell with the lowest current. Therefore, other PV cells also should operate with the lowest current and the system output power is lowered significantly. Even if only one PV cells is shaded and the lowest PV current is dramatically lowered, the system output power is similar with the case when all PV cells are shaded. The power loss generated in the central converter in series configuration $P_{loss,series}$ is calculated as

$$P_{loss,series} = \sum V_{pv} \cdot I_{pv,min} \cdot (1 - \eta_{conv}) \quad (1)$$

where V_{pv} is the PV voltage, $I_{pv,min}$ is the lowest PV current among the PV currents, and η_{conv} is the converter efficiency. Because the central converter processes full PV power, the power conversion loss is also significant.

2) Parallel

In the parallel configuration, PV cells are connected in parallel to a central converter, as shown in Fig. 3(b). Again, each PV cell is not controlled by individual converters such that the system efficiency is lower when there is mismatch in illumination. The PV cell with the lowest voltage limits the operating points of other PV cells. However, since illumination is linked to PV current more than voltage, uneven illumination does not have as large effect on the parallel configuration as the series configuration. The power loss in the central converter in parallel configuration $P_{loss,parallel}$ is calculated as

$$P_{loss,parallel} = \sum V_{pv,min} \cdot I_{pv} \cdot (1 - \eta_{conv}) \quad (2)$$

where $V_{pv,min}$ is the lowest PV voltage among the PV voltages and I_{pv} is the PV current.

3) Cascaded Converter

Cascaded converters are connected to each PV to control the PV cell individually, as shown in Fig. 3(c). Therefore, each cascaded converter can achieve MPPT of the PV cell by processing full PV power. Although there is a mismatch in illumination, each PV cell can operate at own MPP. The total power loss in the cascaded converters $P_{loss,cascaded}$ is defined as

$$P_{loss,cascaded} = \sum V_{pv} \cdot I_{pv} \cdot (1 - \eta_{conv}). \quad (3)$$

Because cascaded converter processes full PV power, the ideal overall system efficiency of cascaded configuration is always identical to the converter efficiency.

4) Series DPP Converters

DPP converters are a more recently introduced concept for PV applications [24-40]. DPP converters also control the PV cells individually like cascaded converters. However, the DPP converter processes only a fraction of the PV power such that it can minimize the power conversion loss generated in converters. One of the fundamental DPP architectures is the series PV-to-bus architecture, as shown in Fig. 4(a). When the DPP converters are connected with PV cells in parallel and PV cells are connected in series, the power loss generated in the DPP converter P_{loss,s_DPP} is defined as

$$P_{loss,s\_DPP} = \sum (I_{string} - I_{pv}) \cdot V_{pv} \cdot (1 - \eta_{conv}) \quad (4)$$

where I_{string} is the string current of the PV system. Eq. (4) can be applied when the string current I_{string} is higher than the PV current I_{pv}. When the string current I_{string} is lower than the PV current I_{pv}, the power loss generated in the DPP converter P_{loss,s_DPP} is defined as

$$P_{loss,s\_DPP} = \sum (I_{pv} - I_{string}) \cdot V_{pv} \cdot (1 - \eta_{conv}) / \eta_{conv}. \quad (5)$$

The power loss generated in the series DPP converter is proportional to the current difference between the string current I_{string} and the PV current I_{pv}. Therefore, when the PV current is similar with the string current, the power loss in DPP converters can be minimized.

5) Parallel DPP Converters

Another fundamental DPP architecture is the parallel DPP configuration, shown in Fig. 4(b). When the DPP converters are connected with the PV cells in series and the PV cells are connected in parallel, the power loss generated in the DPP converter P_{loss,p_DPP} is defined as

$$P_{loss,p\_DPP} = \sum(V_{dc} - V_{pv}) \cdot I_{pv} \cdot (1 - \eta_{conv})/\eta_{conv} \quad (6)$$

where V_{dc} is the dc bus voltage of the PV system. In parallel DPP configuration, the DPP converter output is connected to the PV cell such that the output power of DPP converter is the same with the PV current multiplied by the difference between the dc bus voltage and the PV voltage $|V_{dc} - V_{pv}| \cdot I_{pv}$. Therefore, when the PV voltage is similar with the dc bus voltage, the power loss in DPP converters can be minimized. Usually, the PV voltages are not affected by illumination as much as the PV current, the PV voltages are more constant than the PV current.

C. System Efficiency Comparison of the Five Converter Configurations

The five introduced PV and converter configurations are analyzed and compared for their output performance under the nine different test cases. The system efficiency η_{sys} of each case is defined as

$$\eta_{sys} = (P_{actual} - P_{loss})/P_{ideal} \quad (7)$$

where P_{actual} is the system power actually produced, P_{loss} is the sum of the power losses in all PV system, and P_{ideal} is the ideal system power of the PV system at a given illumination. For the system efficiency calculations, the measured illumination data of 9 usage cases is used for the five converter configurations. For the simplicity, every converter, including DPP converters and the central converter, efficiency is assumed the same and is varied from 70% to 100%, in 5% increments. In total, 45 cases of system efficiencies with seven different converter efficiencies were calculated in Matlab. The maximum power point tracking (MPPT) error is not considered.

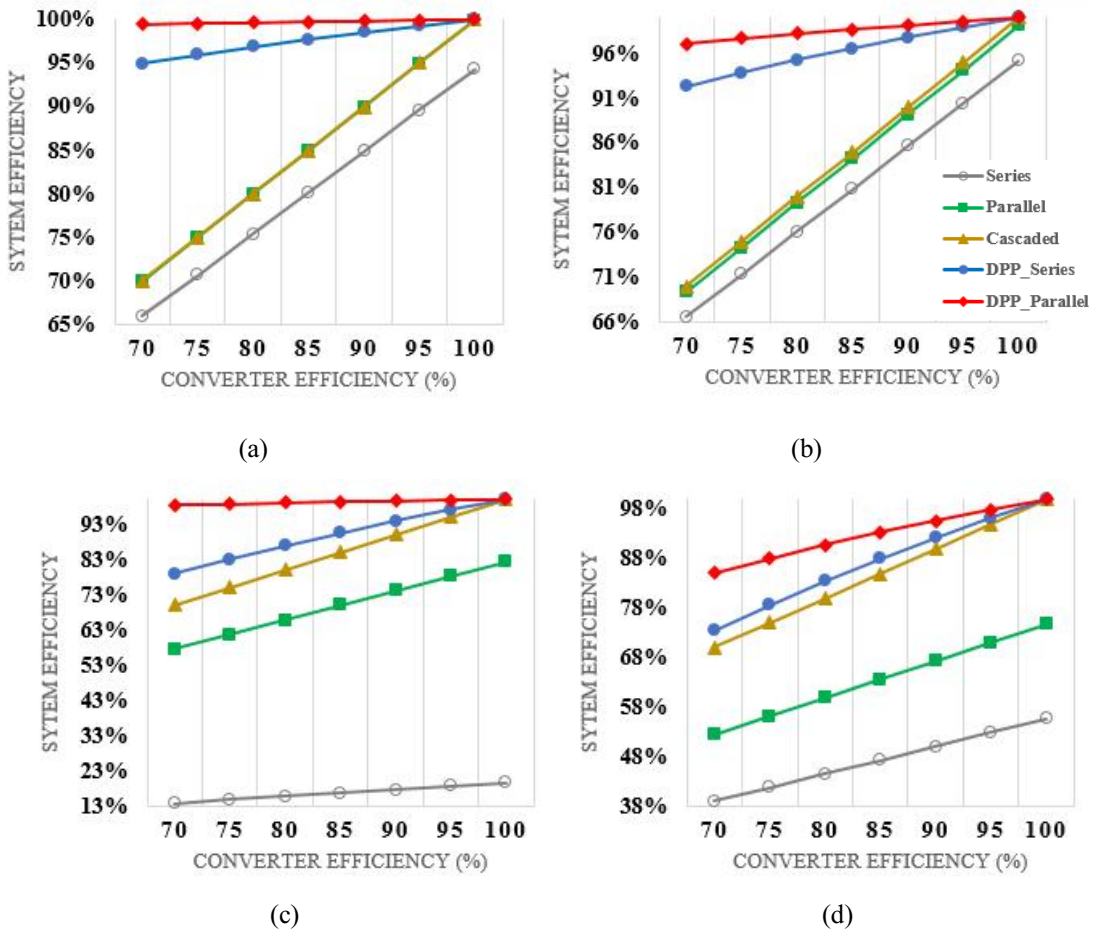

Fig. 7 System efficiency for five different configurations: (a) Case 03, (b) Case 07, (c) Case 05, (d) Case 09.

Fig. 7 shows the system efficiency results for the four usage cases where something is in the bag, making its shape convex. Fig. 7(a) and Fig. 7(b) are non-partial-shading cases, such that the illumination on the PV cells is relatively even. In these cases, traditional converter configurations which are series, parallel, and cascaded configurations show almost same system efficiency with assumed converter efficiency. In series and parallel configurations, the central converter processes full PV power and also cascaded converter processes full PV power. Also, because illumination on PV cells is relatively even in Case 03 and Case 07, the operation points of PV cells are almost same. Therefore, the system efficiency is the same with the assumed converter efficiency. However, DPP configurations show higher system efficiency, more than 95%. Especially, the parallel DPP configuration shows the highest system efficiency and series DPP configuration also shows only slightly lower system efficiency than the parallel DPP configuration. Because illumination is more related with the PV current rather than PV voltage, the processed power in DPP converter is more higher in series DPP configuration than parallel DPP configuration.

Fig. 7(c) and Fig. 7(d) show the partial-shading case results. Because of the partial shading, the differences among the illumination are large, such that the resulting system efficiency varies depending on the configuration. The series configuration shows the lowest system efficiency, 16.63% in Case 05 and 47.24% in Case 09, when the assumed converter efficiency is 85%. The parallel configuration also shows a lower system efficiency compared to the non-partial-shading cases. In the non-partial-shaded cases, the system efficiency of the parallel configuration is almost same as that of the cascaded configuration, but in the partial-shaded cases, it is much lower than the cascaded configuration.

The system efficiency of DPP configurations is the highest in every cases and also it increases proportionally with the converter efficiency. The DPP parallel configuration shows the highest system efficiency in every cases. Because Case 05 assumes that it is a sunny day, the illumination difference between the shaded and non-shaded PV cells is more significant than in Case 09. Thus, the difference between the system efficiency of Case 05 is much bigger than Case 09; the difference is about 83% in Case 05 and 46% in Case 09, when the assumed converter efficiency is 85%. Detailed results for all cases are provided in Table . Overall, the DPP parallel configuration seems the most promising configuration to maximize output power under the irradiance conditions that wearable applications will experience.

TABLE System Efficiency Calculation Results

Case 01	Converter Efficiency	Series	Parallel	Cascaded	DPP Series	DPP Parallel
Ideal	70%	70.00%	70.00%	70.00%	100.00%	100.00%
	75%	75.00%	75.00%	75.00%	100.00%	100.00%
	80%	80.00%	80.00%	80.00%	100.00%	100.00%
	85%	85.00%	85.00%	85.00%	100.00%	100.00%
	90%	90.00%	90.00%	90.00%	100.00%	100.00%
	95%	95.00%	95.00%	95.00%	100.00%	100.00%
	100%	100.00%	100.00%	100.00%	100.00%	100.00%

Case 02	Converter Efficiency	Series	Parallel	Cascaded	DPP Series	DPP Parallel
Sunny, Not Covered, Nothing in Bag	70%	68.77%	69.99%	70.00%	97.56%	99.49%
	75%	73.69%	74.99%	75.00%	98.04%	99.59%
	80%	78.60%	79.99%	80.00%	98.49%	99.68%
	85%	83.51%	84.99%	85.00%	98.90%	99.77%
	90%	88.42%	89.99%	90.00%	99.29%	99.85%
	95%	93.34%	94.99%	95.00%	99.66%	99.93%
	100%	98.25%	99.99%	100.00%	100.00%	100.00%

Case 03	Converter Efficiency	Series	Parallel	Cascaded	DPP Series	DPP Parallel
Sunny, Not Covered, Something in Bag	70%	65.99%	69.97%	70.00%	94.90%	99.44%
	75%	70.71%	74.97%	75.00%	95.91%	99.55%
	80%	75.42%	79.97%	80.00%	96.85%	99.65%
	85%	80.13%	84.96%	85.00%	97.71%	99.75%
	90%	84.85%	89.96%	90.00%	98.52%	99.84%
	95%	89.56%	94.96%	95.00%	99.28%	99.92%
	100%	94.28%	99.96%	100.00%	100.00%	100.00%

Case 04	Converter Efficiency	Series	Parallel	Cascaded	DPP Series	DPP Parallel
Sunny, Covered, Nothing in Bag	70%	15.48%	61.99%	70.00%	89.69%	98.64%
	75%	16.58%	66.42%	75.00%	91.75%	98.92%
	80%	17.69%	70.84%	80.00%	93.63%	99.16%
	85%	18.80%	75.27%	85.00%	95.38%	99.39%
	90%	19.90%	79.70%	90.00%	97.01%	99.61%
	95%	21.01%	84.13%	95.00%	98.55%	99.81%
	100%	22.11%	88.56%	100.00%	100.00%	100.00%

Case 05	Converter Efficiency	Series	Parallel	Cascaded	DPP Series	DPP Parallel
Sunny, Covered, Something in Bag	70%	13.69%	57.58%	70.00%	78.76%	98.36%
	75%	14.67%	61.69%	75.00%	82.99%	98.72%
	80%	15.65%	65.80%	80.00%	86.88%	99.04%
	85%	16.63%	69.91%	85.00%	90.49%	99.32%
	90%	17.61%	74.03%	90.00%	93.85%	99.57%
	95%	18.58%	78.14%	95.00%	97.01%	99.80%
	100%	19.56%	82.25%	100.00%	100.00%	100.00%

Case 06	Converter Efficiency	Series	Parallel	Cascaded	DPP Series	DPP Parallel
Cloudy, Not Covered, Nothing in Bag	70%	67.42%	69.91%	70.00%	92.51%	97.70%
	75%	72.23%	74.90%	75.00%	94.00%	98.16%
	80%	77.05%	79.89%	80.00%	95.37%	98.58%
	85%	81.86%	84.89%	85.00%	96.64%	98.97%
	90%	86.68%	89.88%	90.00%	97.83%	99.34%
	95%	91.49%	94.87%	95.00%	98.94%	99.68%
	100%	96.31%	99.87%	100.00%	100.00%	100.00%

Case 07	Converter Efficiency	Series	Parallel	Cascaded	DPP Series	DPP Parallel
Cloudy, Not Covered, Something in Bag	70%	66.60%	69.36%	70.00%	92.30%	97.05%
	75%	71.36%	74.31%	75.00%	93.83%	97.63%
	80%	76.11%	79.27%	80.00%	95.24%	98.18%
	85%	80.87%	84.22%	85.00%	96.55%	98.68%
	90%	85.63%	89.18%	90.00%	97.77%	99.14%
	95%	90.39%	94.13%	95.00%	98.92%	99.59%
	100%	95.14%	99.09%	100.00%	100.00%	100.00%

Case 08	Converter Efficiency	Series	Parallel	Cascaded	DPP Series	DPP Parallel
Cloudy, Covered, Nothing in Bag	70%	34.06%	50.00%	70.00%	91.74%	96.92%
	75%	36.49%	53.57%	75.00%	93.39%	97.54%
	80%	38.93%	57.14%	80.00%	94.89%	98.10%
	85%	41.36%	60.71%	85.00%	96.30%	98.62%
	90%	43.79%	64.28%	90.00%	97.61%	99.11%
	95%	46.23%	67.85%	95.00%	98.83%	99.56%
	100%	48.66%	71.42%	100.00%	100.00%	100.00%

Case 09	Converter Efficiency	Series	Parallel	Cascaded	DPP Series	DPP Parallel
Cloudy, Covered, Something in Bag	70%	38.90%	52.36%	70.00%	73.37%	85.13%
	75%	41.68%	56.10%	75.00%	78.67%	88.08%
	80%	44.46%	59.84%	80.00%	83.56%	90.82%
	85%	47.24%	63.58%	85.00%	88.07%	93.33%
	90%	50.01%	67.32%	90.00%	92.29%	95.69%
	95%	52.79%	71.06%	95.00%	96.24%	97.91%
	100%	55.57%	74.80%	100.00%	100.00%	100.00%

III. PARALLEL DPP CONVERTERS FOR WEARABLE APPLICATIONS

In this section, the basic concept of the PV-powered bag for simulation and hardware experiments is introduced and power loss in two potential parallel DPP converters configurations are compared.

A. MIC, DC optimizer, and DPP converters

As mentioned, series-connected PV cells are typically connected to a power converter, which controls a PV string using MPPT to optimize output power [9-10]. In the string, all cells must operate on the same current but this current is limited by the PV cell receiving the lowest sunlight. Thus, all PV cells cannot operate at their own MPP when some of the PV cells receive different light intensities and, as a result, output power decreases severely. This power reduction problem commonly occurs in PV systems with long strings of PV cells controlled by one central converter, which has been observed in stationary PV power applications [12], [14–16].

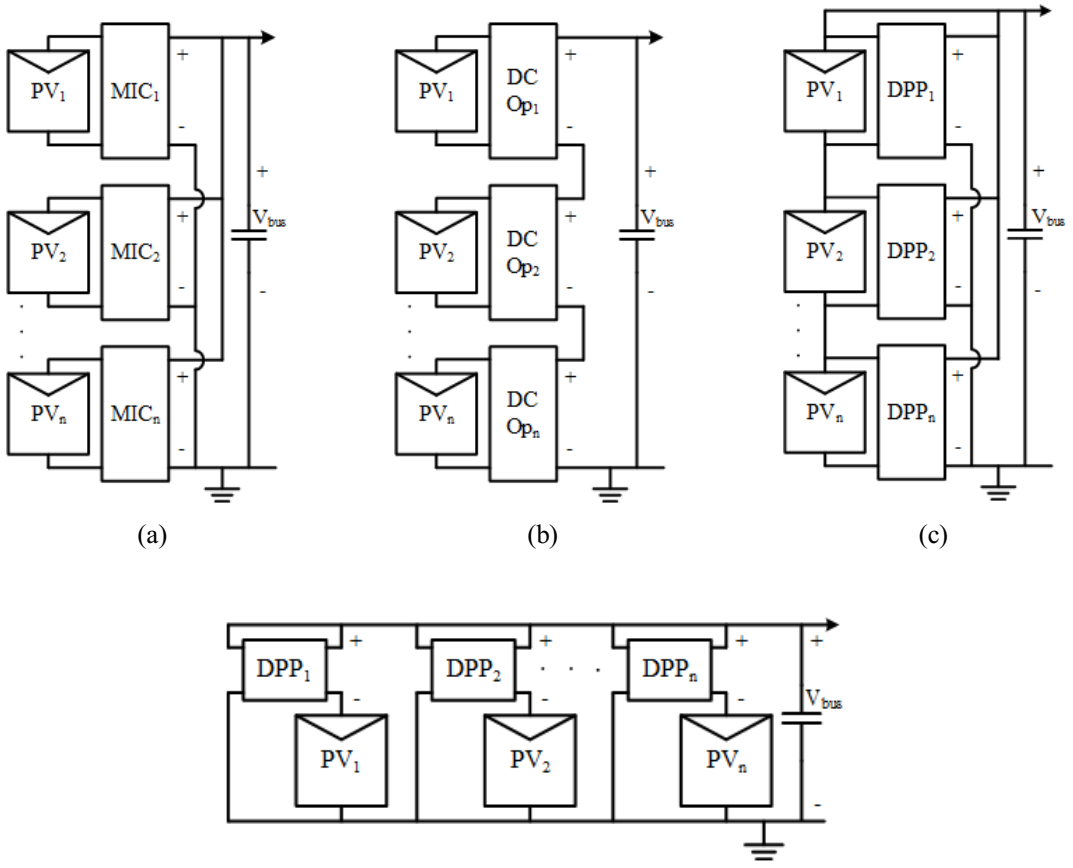

Fig. 8 PV systems with (a) module module-integrated converters (MICs), (b) dc optimizers (cascaded converters), (c) series DPP converters, and (d) parallel DPP converters.

To overcome output power reduction under imbalanced light conditions in series-connected PV systems, various converter architectures have been proposed, such as the module-integrated converter (MIC) [17–19], dc optimizers [20–23], and DPP converters [24-38]. The general MIC architecture is shown in Fig. 8(a). Each MIC is connected to a PV panel such that each PV panel can operate individually and independently. Therefore, each PV panel can operate at its own MPP regardless of the light imbalance among PV cells. However, the PV panel is connected to the grid through the MIC, so the input-output voltage step-up ratio is relatively high. Alternatively, dc optimizers, which is same with the cascaded converter, can be used, as shown in Fig. 8(b). The PV panels are controlled by the dc optimizers, but their outputs are connected in series such that the voltage ratio from dc optimizer output to the grid is lower than for MICs. Still, MICs and dc optimizers are full power processing (FPP) converters [27-28], such that all the PV power passes through the converter and suffers losses before reaching the output.

DPP converters were introduced as a solution that allows for independent MPPT for each PV panel, while only processing a portion of the total PV power. One of the DPP configurations for series-connected PV panels is shown in Fig. 8(c). The majority of the literature on DPP is for series DPP, where the fundamental connection of the PV cells is in series. Series DPP converters are able to compensate for even extreme light differences, but they end up processing a more significant amount of power [8], which takes away from the fundamental advantage of the DPP system. An alternative DPP structure is to use parallel DPP converters, as shown in Fig. 8(d). Based on the operating characteristics of PV cells, the voltage characteristics are less sensitive extreme light differences than the current characteristics [13], [35–37]. This indicates that when extreme light differences are expected, parallel connection is more advantageous for maximizing the power from each cell. Some potential converter topologies for parallel DPP converters have been explored in [38], but the concept and implementation methods still need further investigation.

B. PV-Powered Bag Application

The basic PV-powered bag concept for simulation and hardware is shown in Fig. 1, where PV panels are placed on the outside of a fabric bag and power converters and a charging cable are installed inside the bag. The PV-powered bag consists of four PV cells and each PV cell is controlled by a parallel DPP converter. Each DPP converter controls the PV cell individually and independently using MPPT control. The DPP converters input voltage is the dc bus voltage and the output voltage is the difference between the dc bus voltage and PV cell voltage. The output load, which is a USB-interface mobile device, is connected across the dc bus. A Zener diode is also connected over the dc bus to clamp the dc bus voltage at 5 V, which prevents high voltage from potentially damaging the load.

Wearable applications cannot avoid lighting mismatch. If a traditional series string configuration is implemented, the output power will be extremely low due to the sunlight mismatch. This mismatch problem can be overcome in the power converter system design using DPP converters. It was found that parallel DPP converter configuration, as shown in Fig. 8(d), exhibits the highest system efficiency among several configurations in various realistic cases. This configuration maximizes the system output with the highest overall system efficiency even under imbalanced light conditions.

There are multiple approaches to implementing parallel DPP converters. Authors in [38] explore both the flyback and inverted (low-side switch) buck converter in two main architectures for the parallel DPP converter system: with and without a front-end converter. For this low-voltage wearable application, the inverter buck converter is chosen because it allows for high efficiency and small size. However, the decision to use a front-end converter or not is not as apparent and requires comparative analysis to determine the best approach. The proposed power system without a front-end converter is shown in Fig. 9(a), while the system with a front-end converter is shown in Fig. 9(b).

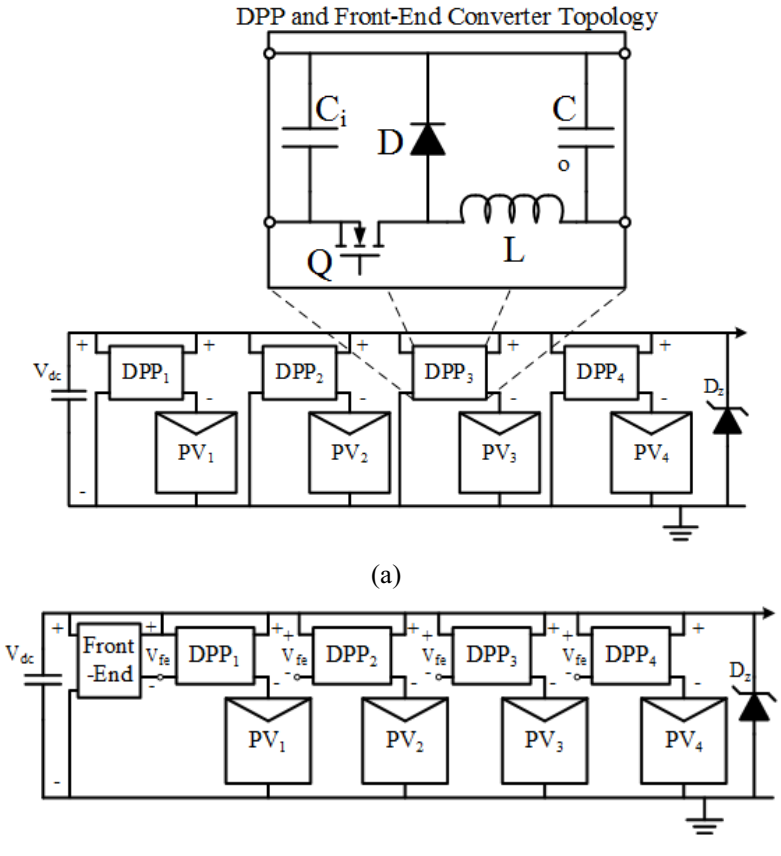

Fig. 9. System schematic using parallel DPP buck converters (a) without and (b) with a front end converter.

C. Parallel DPP System Analysis

For the parallel DPP architectures, shown in Fig. 9, the power loss generated in a DPP converter is provided in (5). According to (5), when the voltage difference between V_{dc} and V_{pv} is small, the power loss is also small. For the parallel DPP architecture with a front-end converter, shown in Fig. 9(b), the power loss in the front-end converter is

$$P_{loss,fe} = \frac{(1-\eta_{fe})}{\eta_{fe}\cdot\eta_{conv}} \sum_{i=1}^{n} (V_{dc} - V_{pv,i}) \cdot I_{pv,i} \tag{6}$$

where η_{fe} is the efficiency of the front-end converter. For simplicity, it is assumed that the efficiency of the DPP and front-end converter are the same.

As an example, assume the light intensity conditions shown in Fig. 11, where the intensity is different for each PV cell. Each PV is controlled by the DPP converter to operate at its individual MPP voltage, which changes depending on the light intensity, as shown in Fig. 10. Assume that V_{dc} is 5 V and conv is 80% and does not vary with load. The PV voltage and current values are based on datasheet values of the PV cells used in the design. In Fig. 11(b), the front-end converter output voltage is 2 V.

To illustrate the advantages of parallel DPP architectures, the power losses for the MIC (FPP), DPP parallel without a front-end converter, and DPP parallel with a front-end converter systems are compared based on the example setup given in Fig. 11. The PV voltages and currents were calculated based on the different irradiance levels using a PV model implemented in Matlab. The resulting voltages are shown in Fig. 11 and the current are 0.25, 0.20, 0.12, and 0.04 A for PV 1, 2, 3, and 4, respectively.

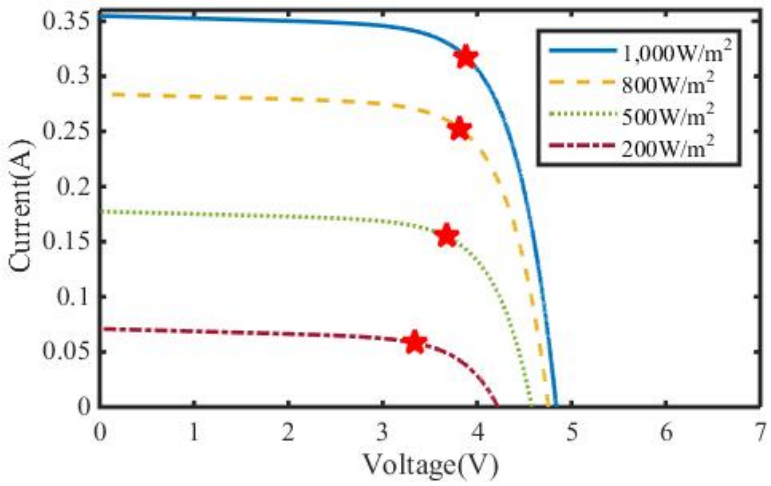

Fig. 10 PV I-V characteristics with different sunlight intensities

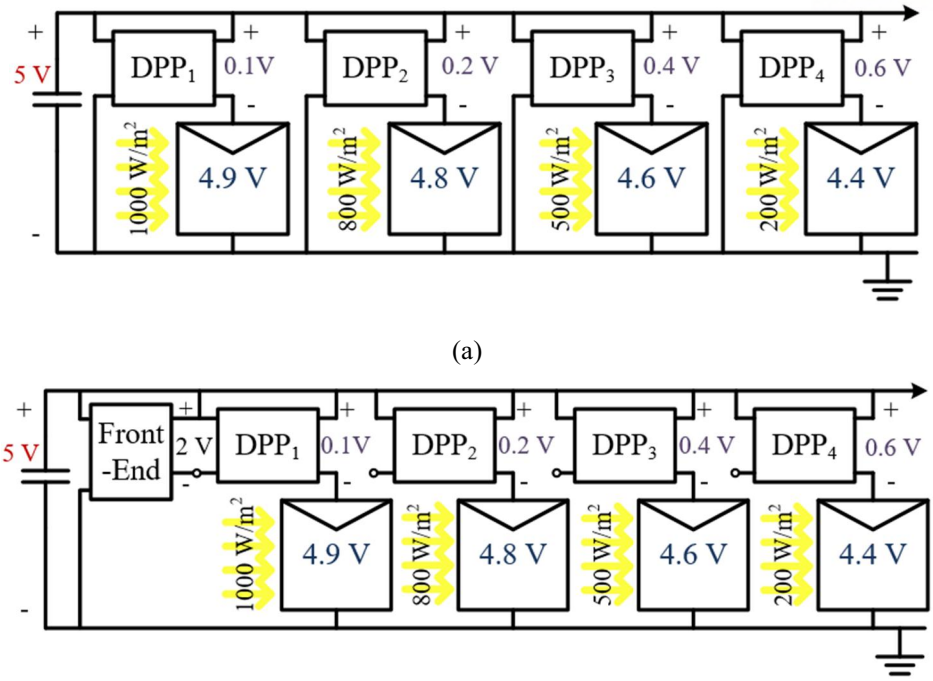

Fig. 11. Example irradiance conditions showing PV and converter voltages (a) without and (b) with a front end converter.

TABLE □ Power Loss Comparison for Parallel MIC and DPP converter with and without front-end converter

Parallel MIC (FPP)			
PV	$P_{conv,fpp}$ (W)	$P_{loss,fpp}$ (W)	$P_{loss,tot}$ (W)
1	1.23	0.25	**0.59**
2	0.96	0.19	
3	0.57	0.11	
4	0.19	0.04	

Parallel DPP Converters			
PV	$P_{conv,dpp}$ (W)	$P_{loss,dpp}$ (W)	$P_{loss,tot}$ (W)
1	0.05	0.01	**0.04**
2	0.05	0.01	
3	0.05	0.01	
4	0.03	0.01	

Front-End Converter			
Converter	$P_{conv,fe}$ (W)	$P_{loss,fe}$ (W)	$P_{loss,tot}$ (W)
Front-end	0.23	0.05	**0.08**

Table shows the power loss comparison between parallel MIC (FPP) and DPP converter architectures. Under the given sunlight condition, it is assumed that every PV cell operates at its own MPP. However, the MICs process 100% of the PV power such that the total power loss in the MICs is much higher than the DPP converters. Conversely, DPP converters process only a small fraction of PV power such that the total power loss in the DPP converters is 15 times smaller than MICs. Although the produced power from the PV cells are the same in all cases, the system output power in the parallel DPP systems are significantly higher than the MIC system. Between the two parallel DPP configurations, the system with the front-end converter has an additional power conversion stage, which increases overall losses. However, the additional voltage stage allows the output of the DPP converter to properly operate at very low voltages.

IV. SYSTEM DESIGN ANALYSIS

The design choices for the power system are driven by the characteristics of the battery load and PV cells, which are analyzed in this section. The select the most appropriate DPP configuration, the two parallel configurations with and without a front-end converter are compared in detail.

A. Battery Impedance

The target load for the PV-powered bag is a Li-ion battery in a portable battery or mobile device at a nominal 5 V. However, the charging characteristics and impedance of the battery depend on the battery state of charge (SOC). When charging the battery, the battery impedance affects to dc bus voltage of parallel DPP system. In the PV-powered bag application, dc bus voltage is clamped by a Zener diode to prevent the dc bus from exceeding 5 V, which would could damage the load or the converter circuitry. Thus, the bus voltage will not exceed 5 V, but charging can occur at lower voltages, depending on the battery impedance.

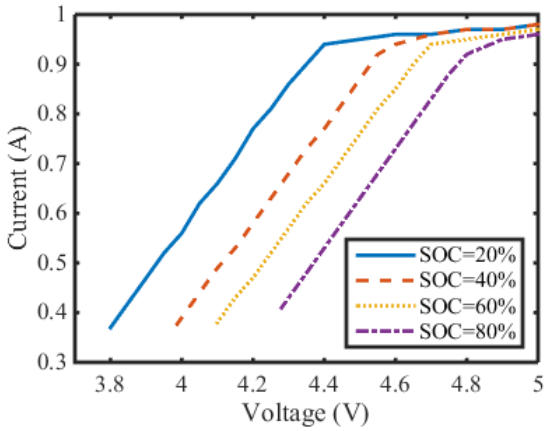

Fig. 12. Portable battery charging voltage and current characteristics measured at different SOC values.

In this design, a 6,500 mAh portable battery is used as the load and its measured charging characteristics are shown in Fig. 12. As shown, the output current must be larger than 0.4 A to begin charging the battery. The minimum charging voltage decreases with decreasing SOC. At 20% SOC the dc bus voltage must exceed 3.8 V to begin charging at 0.37 A, which is 1.4 W of power. Based on the DPP parallel topology, the PV voltage must always be lower than dc bus voltage. Note that if the MPP of the PV cell is higher than the dc bus voltage, MPPT is not achieved and PV cells may not generate sufficient power to charge the battery. Thus, in order to charge the battery at lower SOC and at lower input power levels (lower lighting conditions), a PV cell with a maximum power point at or below 3.8 V should be selected.

However, the power loss in DPP converters is proportional to the voltage difference between V_{dc} and V_{pv}, according to (5). From a power-loss perspective, it is better to have the PV cell MPP voltage slightly lower than dc bus voltage, which is normally 5 V. However, this means that the system may not be able to charge the battery when it is at low SOC or at low input power conditions. This is a fundamental trade-off between charging capability and power loss, which will be further investigated in this work.

B. PV Cell Selection

As mentioned, the MPP voltage of the PV cells affects the battery charging voltage range and the system power efficiency. Under nominal sunlight when there is sufficiently high input power, the total system power is enough and dc bus voltage would be close to 5 V. When the PV voltage at MPP is similar with dc bus voltage, power loss in DPP converters can be minimized. However, if the weather is cloudy or if there is partial shading, the total system power is low and MPP is too high to charge the battery with at the low input power level. Because buck converters are used for DPP converters in PV-powered charging bag, dc bus voltage should be bigger than PV voltages. If dc bus voltage is lower than PV voltages at MPP, PV cells can still produce power but not at MPPT. Then, the total system power might be much lower under the given sunlight condition, such that the PV-powered bag cannot charge the battery.

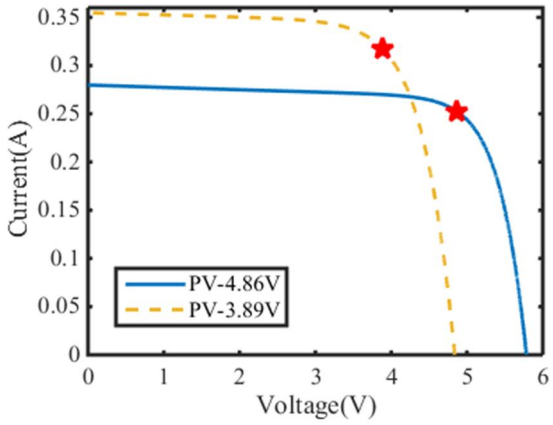

Fig. 13. I-V curves for two PV cells with different MPP values.

Here, two design approaches are considered: 1) with the PV MPP voltage close to the nominal dc bus voltage and 2) with a lower MPP voltage near the minimum charging voltage value. Two PV cell types with different MPP voltages are selected, as shown in Fig. 13. The two PV cells have the same maximum power of 1.23 W under nominal sunlight, but have different I-V characteristics and MPP represented as red star in Fig. 6. The first PV has a nominal MPP at 4.86 V and 0.25 A, such that the MPP voltage is close to the with 5 V dc bus voltage. The second PV has a MPP at 3.89 V and 0.32 A, such that PV MPP voltage is closer to the 3.8 V minimum charging voltage.

C. Parallel DPP Architecture Selection

Two parallel DPP architectures, with and without a front end converter, were introduced in Section 3. The appropriate DPP architecture depends on the MPP voltage of the selected PV cells. If the 4.86-V PV cell is selected and the DPP architecture without the front-end converter is used, the nominal output voltage of the DPP converter is 0.14 such that the step-down voltage ratio is 0.03. This small duty ratio can lead to control difficulties. Therefore, the parallel DPP system with a front-end converter is used, as shown in Fig. 11(b), for the higher-voltage PV cell. The front-end buck converter steps down the dc bus voltage to 2 V and the front-end converter output is connected to the input of each DPP converters. Then, the DPP converters step down from 2 V to the voltage difference between V_{dc} and V_{pv}.

If the 3.89-V PV cell is selected and the DPP architecture without the front-end converter is used, the nominal output voltage of the DPP converter is 1.11 V such that the step-down voltage ratio is 0.22. This duty ratio is more manageable such that a front-end converter is not needed. Thus, the parallel DPP architecture with a front-end converter is used for the lower-voltage PV cell.

D. Parallel DPP Configuration Comparison

Next, the two parallel DPP designs are analyzed to compare their performance under various conditions. Six irradiance test cases are chosen for the four PV cells, which are outlined in Table . Case 1 represents a sunny day with only slight variation across the cells, to emulate when the bag face is flat. Case 2 represents a sunny day but with more significant variation across the panels, to emulate when the bag face is rounded. Case 3 represents a sunny day with one PV cell heavily shaded, emulating when something is partially blocking the bag face. Cases 4, 5, and 6 are the same conditions as Cases 1, 2, and 3, respectively, but for a partially cloudy day.

TABLE Irradiance Scenarios

Case	PV 1	PV 2	PV 3	PV 4
01	1,000 W/m^2	1,050 W/m^2	900 W/m^2	950 W/m^2
02	1,000 W/m^2	700 W/m^2	500 W/m^2	200 W/m^2
03	1,000 W/m^2	1,050 W/m^2	900 W/m^2	50 W/m^2
04	500 W/m^2	550 W/m^2	400 W/m^2	450 W/m^2
05	500 W/m^2	400 W/m^2	300 W/m^2	150 W/m^2
06	500 W/m^2	550 W/m^2	450 W/m^2	50 W/m^2

The six irradiance test cases were implemented in Matlab to determine their total system power and efficiency. Parallel DPP system with a front-end converter uses the higher-voltage PV cells (4.86 V/0.25 A) and the system without a front-end converter uses the lower-voltage PV cells (3.89 V/0.32 A). The PV cells are modeled using a basic PV model implemented in Matlab [36]. For a direct comparison, the converter efficiency of both the front-end converter and DPP converters are assumed to be 80%. The battery at SOC 20% is used as the output load, such that dc bus voltage changes depending on the battery impedance and system output power. Note that if MPPT is not working because the dc bus voltage is lower than the cell MPP, it is assumed that the corresponding DPP converter are tuned off such that there are no power losses in the converter.

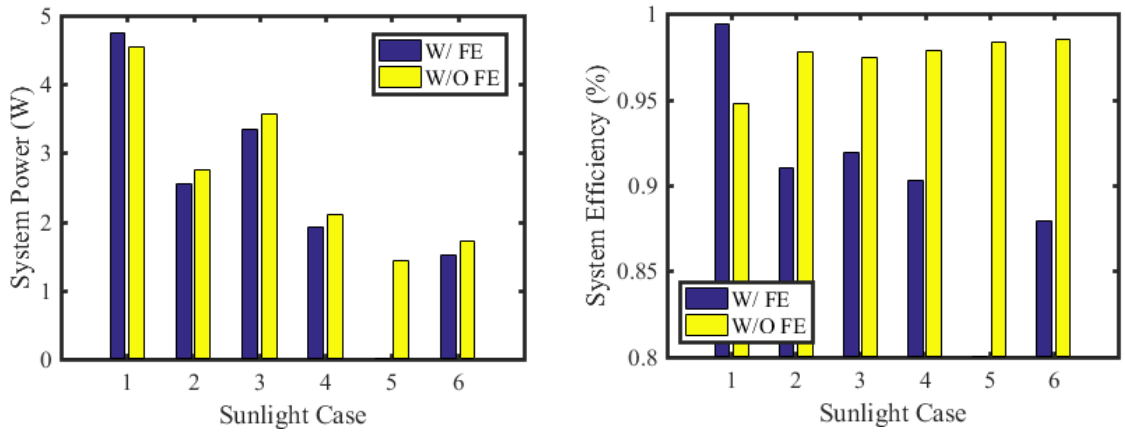

(a) (b)

Fig. 14. System output power (a) and system efficiency (b) under each irradiance case of parallel DPP system with and without front-end converter.

Fig. 14 shows the results of the simulation for each case, comparing the two different parallel DPP designs. Fig. 14(a) shows the system output power for each case and Fig. 14(b) shows overall system efficiency, actual output power over the MPP PV power. The system with the front-end converter shows the higher output power and system efficiency for Case 1, when the cells receive near nominal power and fairly uniform light. This is because the higher-voltage PV cell voltages are close to the dc bus voltage under nominal irradiance, such that very little power is processed through the DPP converters. However, the parallel DPP design without a front-end converter shows higher system power and higher efficiency for the remaining cases. This is because Cases 2 to 6 represent situations where the dc voltage bus must be lower to properly charge the battery load at the lower input power level. In these cases, the lower-voltage PV cells operate closer to their MPP and differential power only needs to be processed through one power stage, the DPP converter. Note that in Case 5, the required dc bus voltage for the front-end converter design is lower than the minimum charging voltage for the battery such that it cannot charge. Performance aspects for both designs are compared in Table .

TABLE Performance Comparison of DPP Configurations

Aspect	With FE	Without FE
MPPT with low dc bus	fair	good
Charging at low input power	fair	good
System power: nominal, uniform	excellent	good
System power: lower or non-uniform	poor	good

If the irradiance conditions are at nominal and uniform irradiance, the higher-voltage PV cells with a front-end converter is the better design. However, the PV-powered bag application will frequently experience uneven lighting and partial shading. From a usability perspective, it is best to ensure that the system can charge the battery over a wide range of lighting conditions. Therefore, the lower-voltage PV cells and parallel DPP system without a front-end converter is the more appropriate design for the PV-powered bag.

V. SIMULATION

To investigate parallel DPP system without a front-end converter using the lower-voltage PV cells, dynamic simulations are setup in PSIM. The circuit diagram is as shown in Fig. 9(a) and component values are provided in Table . Perturb and observe (P&O) method is used for MPPT, with a voltage step size of 0.1 V. PV models are designed using the 'Solar module (physical model)' function in PSIM with the same specifications as given in Fig. 13. The switching frequency is 100 kHz and MPPT frequency is 5 Hz. At first, all PV cells receive 1,000 W/m^2 irradiance but after 1.2 seconds, irradiance is changed to 800 W/m^2, 500 W/m^2, and 200 W/m^2 for PV 2, 3, and 4, as shown in Fig. 15(a).

TABLE Design Component Values

Part	Value
dc bus capacitor	220 μF
DPP converter input capacitor	47 μF
DPP converter output capacitor	62 μF
DPP converter inductor	2.7 μH
DPP converter diode	PMEH1020EJ
Zener diode	1N5338B
MOSFET	2N7002P
signal isolator	ISO7420
gate driver	ZXGD3005E6TA
f_{sw}	100 kHz

The simulation results of the PV voltages are shown in Fig. 15(b), along with the dc bus voltage and power in Fig. 15(c). After the irradiance change, each DPP converter adjusts the voltage to reach the new MPP for each cell independently. Also, the dc bus voltage lowers to match the battery load characteristics at the lower system power. Even though the dc bus voltage is under 5 V, the portable battery load can still be charged. After each PV cell reaches its new MPP, the actual system power returns to the new ideal system power, as shown in Fig. 15(c). These simulation results validate that the parallel DPP system properly achieves MPPT and adjusts quickly to imbalanced lighting conditions.

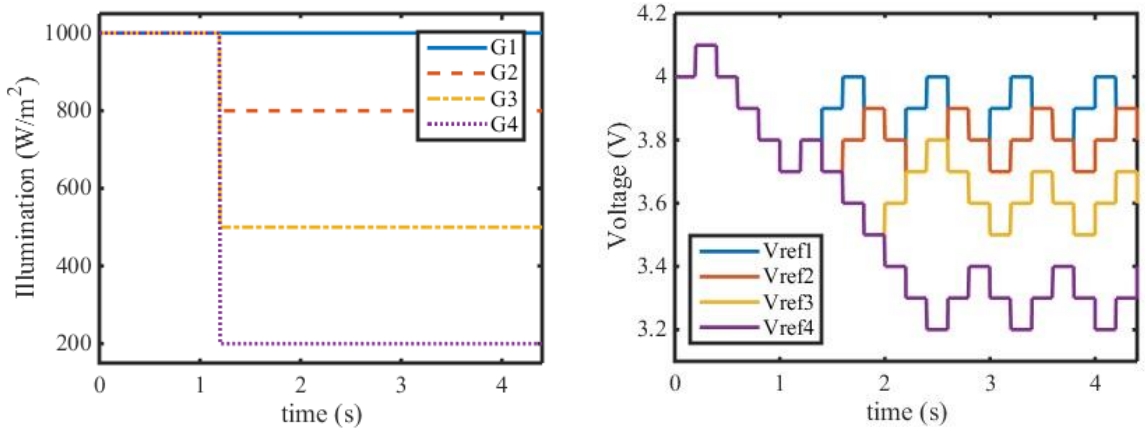

(a)

(b)

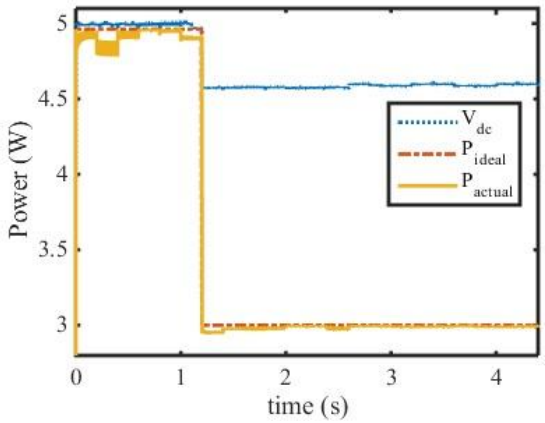

(c)

Fig. 15. (a) Change of illumination on PV cells, (b) MPPT PV voltage references, and (c) the DC bus voltage and system power simulation results for the parallel DPP system

VI. FIRST PROTOTYPE EXPERIMENT

A. Hardware Setup

The experimental setup for the first prototype is shown in Fig. 16(a) and the hardware prototype is shown in Fig. 16(b). In Fig. 16(a), two lamps were used to provide different illumination on the PV cells. During the experiment, lamp2 provided stronger illumination on PV 3 and PV 4. PV 1 and PV 2 received about 300 W/m^2 and PV 3 and PV 4 received about 500 W/m^2. For easy of troubleshooting, the PCB size is larger than necessary and minimized in a later prototype version. Also, in the next prototype, the front-end converter and all four DPP converters is combined onto one PCB. The MPPT frequency is about 0.4 Hz and the detail converter design specifications for the first hardware prototype are provided in Table Ⅶ.

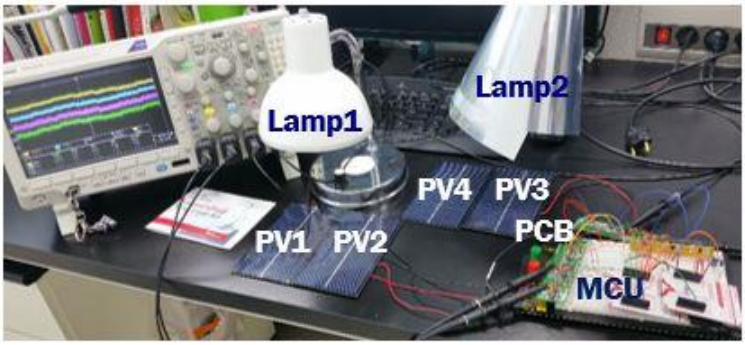

(a)

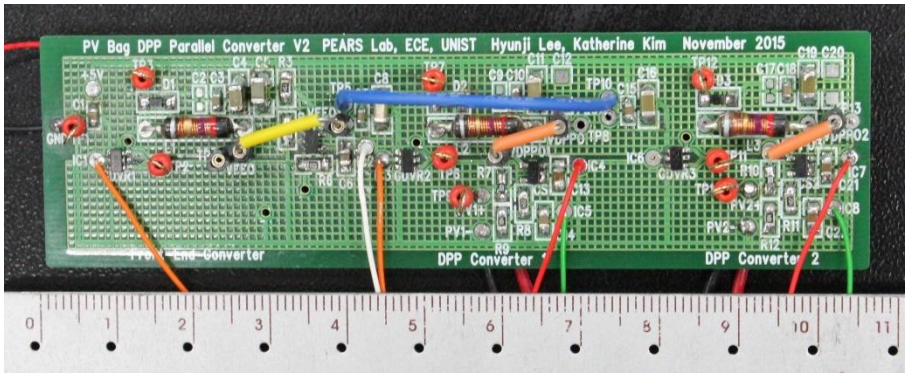

(b)

Fig. 16. (a) Experiment setup and (b) The size of one PCB.

B. Experimental Results

Fig. 17 shows the voltage signal of the PV system with two DPP converters. The top blue line represents the dc bus voltage clamped by the Zener diode at 5 V and the second light-blue line represents the low side of the front-end converter output which is the node shown with a blue line in Fig 16. To make the front-end converter output 2 V, the low side of the front-end converter output, relative to ground, should be 3 V. Voltage control is implemented such that that target voltage difference between the dc bus voltage and low side of the output is 2 V. In other words, the front-end converter output voltage will be 2 V even if the dc voltage is not exactly 5 V. The third purple line and fourth green line represent the PV voltage for two different cells. In the P&O algorithm, once the MPP is found the algorithm follows a repeated 3-step sequence around the MPP value. The voltage waveforms shown in Fig. 17. exhibit this 3-step pattern, meaning that the two voltages are independently controlled at their respective MPP.

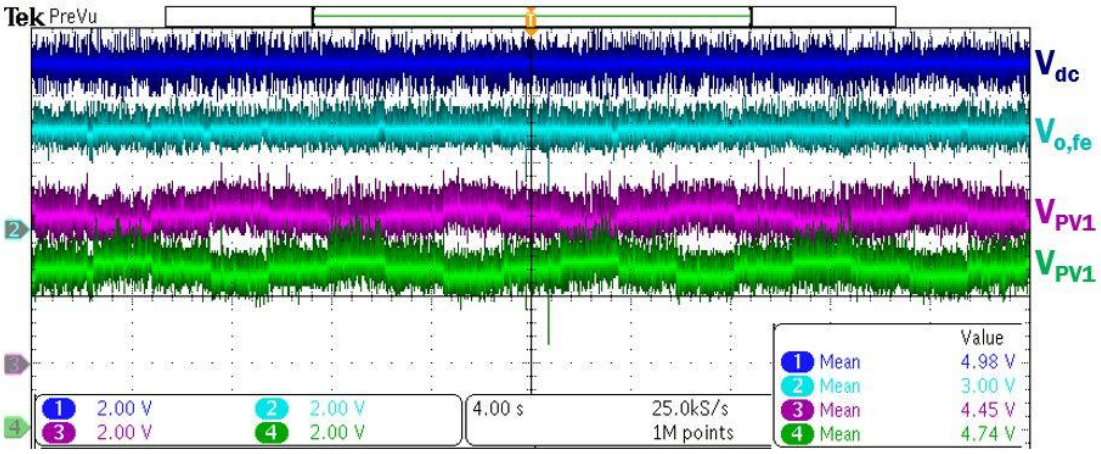

Fig. 17. Experiment results with two DPP converters.

In order to show the benefit of DPP converter, the DPP parallel architecture and direct parallel connection without DPP are compared experimentally. The dc bus voltage and the system output current are measured under same illumination condition to compare output power with and without DPP. Two PV cells are used and the illumination on both cells is about 300 W/m^2. For the parallel PV system, the same PCB with the DPP converters and front-end converter is used but all converters are turned off.

Fig. 18(a) shows the system output power of parallel-connected PV system. The top blue line represents the dc bus voltage, the second light-blue line, and third purple line represent the PV voltages of two PV cells. Because there is no converter, the PV voltages are determined by the load, which is a mobile device. The fourth green line represent the system output current, 23.1 mA and the fifth red line represents the system output power, which is calculated through the Math function in the oscilloscope. The average system output power for the parallel PV system is 114 mW.

Fig. 18(b) shows the system output power with two DPP converters and the front-end converter. The two PV voltage waveforms show the MPPT three-step voltage sequence properly tracking the MPP and the system output current is 40.3 mA, such that the average system output power is 203 mW. While there is no converter in the parallel connected PV system, the DPP parallel system has three converters that results in some converter power loss. However, as shown in Fig. 18, the parallel DPP converter significantly increase the output power, by 78%, compared to without the DPP converters. Through the experiments, the parallel DPP converter control and independent MPPT operation was validated and higher system output power with DPP converters was shown.

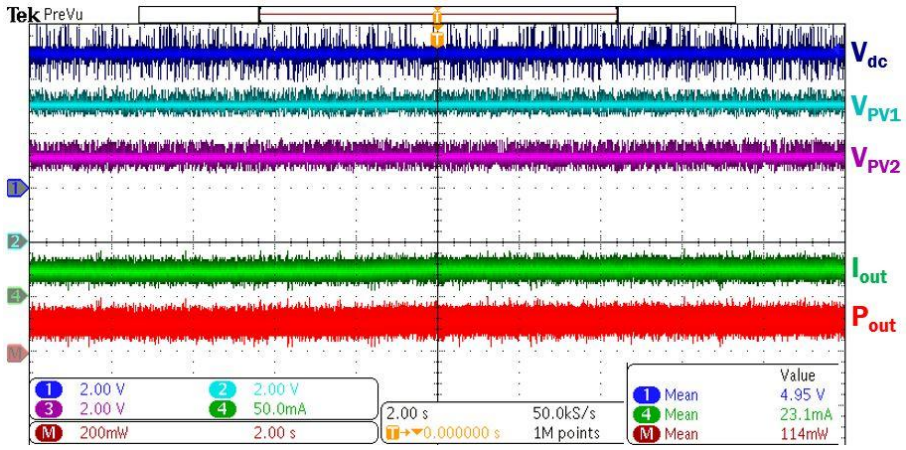

(a)

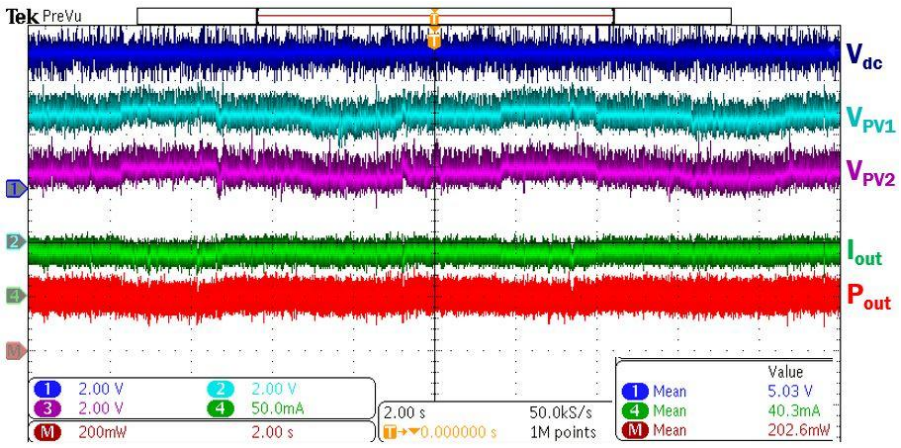

(b)

Fig. 18. System output power (a) without and (b) with two DPP converters

VII. SECOND PROTOTYPE EXPERIMENT

In this section, the experiment results with updated second prototype is explained.

A. Hardware Setup

The experimental prototype is also developed to validate the performance of the parallel DPP system. The PCB is shown in Fig. 19(a) and the experimental setup is shown in Fig. 19(b). The PCB consists of the power stage for the four DPP converters, signal isolators, gate drivers, voltage sensor circuits, Zener diodes for protection, and a dc bus voltage capacitor. The converters are controller using a low-power microcontroller, which measures the PV cell voltage and current, and drives the gate of the corresponding DPP converter through a signal isolator circuit. Zener diodes clamp dc bus voltage to 5 V to protect the load. The P&O MPPT frequency is 1 Hz. Detailed component information is provided in Table □.

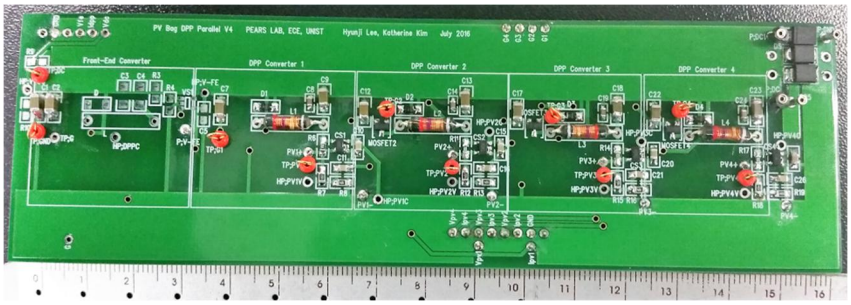

(a)

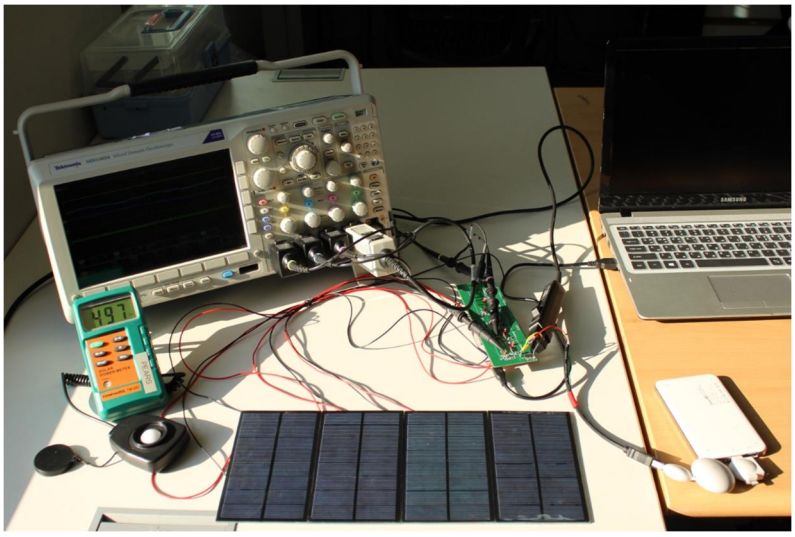

(b)

Fig. 19. (a) The PCB and (b) experimental setup for the hardware prototype.

B. Experimental Results

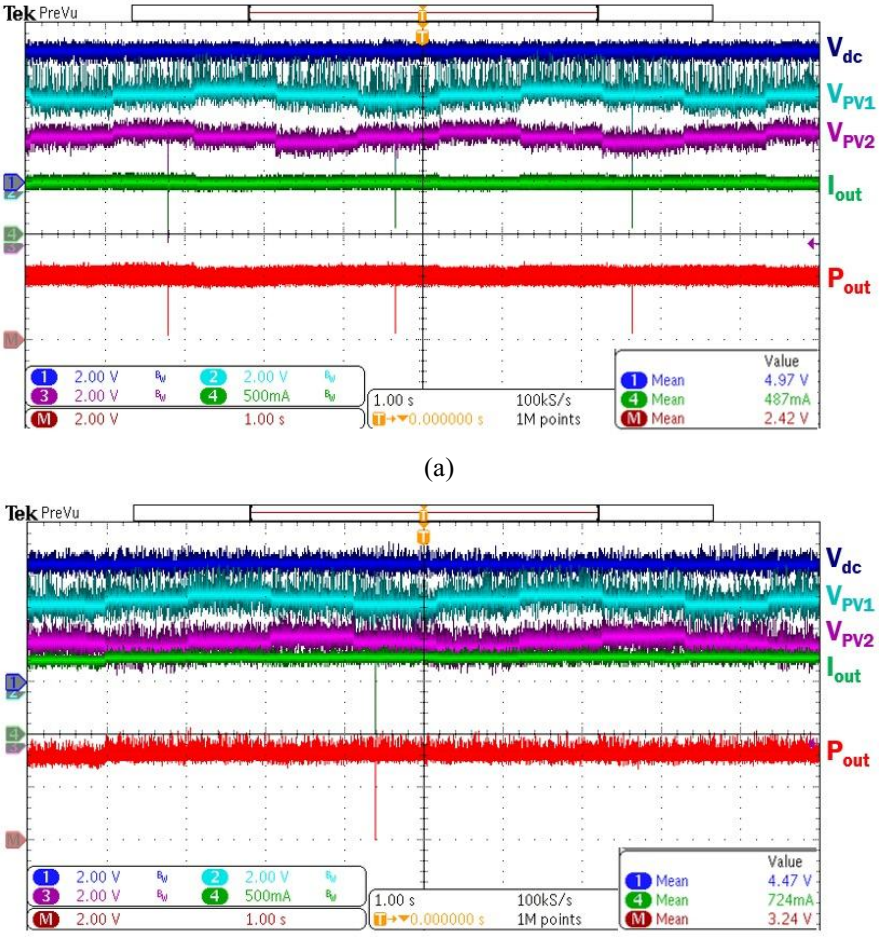

Fig. 20. Experimental waveforms for the DPP system (a) clamped at 5 V and (b) charging a battery.

Fig. 20 shows experimental waveforms for the parallel DPP system prototype under approximately nominal irradiance of 1,000 W/m^2. In these figures, the top blue line is dc bus voltage, the second light-blue line is PV1 voltage, the third purple line is PV2 voltage, the forth green line is output current, and the fifth red line is system output power. Fig. 20(a) shows the experimental system when the dc bus voltage is clamped at 5 V by the Zener diodes. Independent MPPT is achieved for each PV, which is shown by the PV voltages stepping up and down in a repeating three-step pattern. Since the dc bus voltage is 5 V, there are some losses in the DPP converters such that the system output power is only 2.42 W. Fig. 20(b) shows the experimental system waveforms while charging the battery load. Again, the PV voltages show proper MPPT, but the dc bus voltage is 4.47 V because the output must match the battery impedance. Because the dc voltage is closer to the MPP of the PV cells, there are fewer losses in the DPP converters, resulting in a higher system output power of 3.24 W. These experimental hardware results validate the normal operation of the parallel DPP system achieving MPPT and charging the target battery load.

C. Efficiency

Previous analysis assumed a constant converter efficiency of 80%, but the converter efficiency varies with power level and output voltage. Fig. 12 shows the DPP converter efficiency with 5-V input voltage and output voltages are 2 V and 0.5 V. For all six test cases in Table , the power processed in DPP converter for the system without a front-end converter is less than 0.33 W. When the output voltage is 2 V, as shown in Fig. 21(a), the efficiency below 0.3 W is above 80%. When the output voltage is 0.5 V, as shown in Fig. 21(b), the efficiency decreases more drastically as power increases. Mainly, this power loss is from the Schottky diode voltage drop in DPP buck converter that is more prominent at low output voltages. The converter efficiency can be improved using other converter types, such as a synchronous buck converter, in future work.

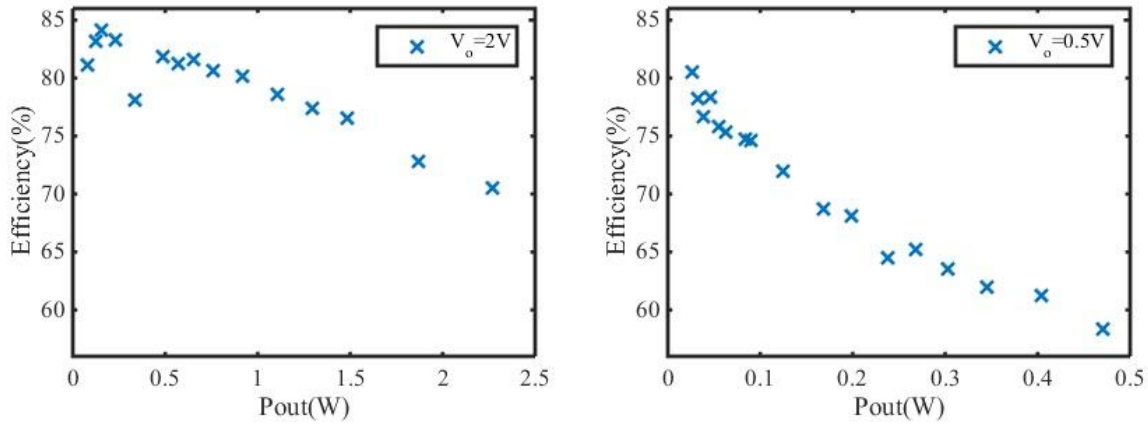

(a) (b)

Fig. 21. DPP converter efficiency with (a) 5-V input voltage 5 V and output voltage of 2 V and (b) output voltage of 0.5 V.

VIII. CONCLUSION

In this thesis, a PV-powered bag using parallel DPP converters is explored through mathematical analysis, simulation, and hardware experiments. The PV-powered bag is a wearable application that can charge a portable battery or mobile device using photovoltaic power. To get optimized system operation of the PV-powered bag, the system efficiency analysis of nine usage test cases and five PV and converter configurations were conducted in Matlab. In all usage cases, the DPP parallel configuration showed the highest system efficiency such that parallel DPP converter is adapted for the PV-powered bag. It consists of four PV cells, each independently controlled by a parallel DPP converter.

To optimize system operation over a range of potential sunlight conditions, two parallel DPP systems using the buck converter topology were compared: parallel DPP system with and without a front-end converter. The parallel DPP system with a front-end converter uses higher-voltage PV cells such that the power loss generated in DPP converters is relatively small under nominal irradiance conditions. However, it cannot always achieve MPPT when the dc bus voltage is low, such that it cannot charge the battery load in some irradiance cases. The parallel DPP system without a front-end converter uses lower-voltage PV cells, such that the power loss generated in DPP converters is slightly higher in nominal irradiance conditions but it shows higher system efficiency at lower dc bus voltages and is able to charge the battery load over a wider range of irradiance conditions. Thus, the parallel DPP system without a front-end converter design is selected for the PV-powered bag application. MPPT and proper charging of the battery load is verified through simulation and experimental results. Future work will focus on minimization of the PCB, improving DPP converter efficiency, and adapting the circuit for a flexible PCB implementation.

REFERENCES

[1] H. Pandey, I. Khan, A. Gupta, “Walking based wearable mobile phone charger and lightening system”, in Proc.MedCom. Intl. Conf. Medical Imaging, pp. 407-411, Nov. 2014.

[2] B. Akin, “Solar Power Charger with Universal USB Output”, in Proc. IEEE Intl. Conf. Power Electron., India, pp. 1-4, Dec. 2012.

[3] B.C. Babu, S. Sriharsha. A. Kumar, N. Saroagi, S.R. Samantaray, “Design and Implementation of Low Power Smart PV Energy System for Portable Applications using Synchronous Buck Converter”, in International Symp. Electron. System Design, pp. 260-266, Dec. 2011.

[4] Q. Brogan, T. O'Connor and D. S. Ha, "Solar and thermal energy harvesting with a wearable jacket," 2014 IEEE International Symposium on Circuits and Systems (ISCAS), Melbourne VIC, 2014, pp. 1412-1415.

[5] P. Vithayasrichareon, G. Mills and I. F. MacGill, "Impact of Electric Vehicles and Solar PV on Future Generation Portfolio Investment," in IEEE Transactions on Sustainable Energy, vol. 6, no. 3, pp. 899-908, July 2015.

[6] K. W. Hu and C. M. Liaw, "Incorporated Operation Control of DC Microgrid and Electric Vehicle," in IEEE Transactions on Industrial Electronics, vol. 63, no. 1, pp. 202-215, Jan. 2016.

[7] P. Manganiello, M. Balato, and M. Vitelli, “A survey on mismatching and aging of pv modules: The closed loop,” IEEE Transactions on Industrial Electronics, vol. 62, no. 11, pp. 7276–7286, Nov. 2015.

[8] K. A. Kim, P. S. Shenoy, and P. T. Krein, “Converter rating analysis for photovoltaic differential power processing systems,” IEEE Trans. Power Electron., vol. 30, no. 4, pp. 1987–1997, Apr. 2015.

[9] C. Barth and R. C. N. Pilawa-Podgurski, “Dithering digital ripple correlation control for photovoltaic maximum power point tracking,” IEEE Transactions on Power Electronics, vol. 30, no. 8, pp. 4548–4559, Aug. 2015.

[10] S. Moon, S. G. Yoon, and J. H. Park, “A new low-cost centralized MPPT controller system for multiply distributed photovoltaic power conditioning modules,” IEEE Transactions on Smart Grid, vol. 6, no. 6, pp. 2649–2658, Nov. 2015.

[11] L. Gao, R. A. Dougal, S. Liu, and A. P. Iotova, “Parallel-connected solar pv system to address partial and rapidly fluctuating shadow conditions,” IEEE Transactions on Industrial Electronics, vol. 56, no. 5, pp. 1548–1556, May 2009.

[12] C. Olalla, C. Deline, and D. Maksimovic, “Performance of mismatched pv systems with submodule integrated converters,” IEEE Journal of Photovoltaics, vol. 4, no. 1, pp. 396–404, Jan. 2014.

[13] K. A. Kim and P. T. Krein, “Reexamination of photovoltaic hot spotting to show inadequacy of the bypass diode,” IEEE J. Photovoltaics, vol. 5, no. 5, pp. 1435–1441, Sept. 2015.

[14] D. Debnath, P. De, and K. Chatterjee, “Simple scheme to extract maximum power from series connected photovoltaic modules experiencing mismatched operating conditions,” IET Power Electronics, vol. 9, no. 3, pp. 408–416, 2016.

[15] H. S. Sahu, S. K. Nayak, and S. Mishra, “Maximizing the power generation of a partially shaded pv array,” IEEE Journal of Emerging and Selected Topics in Power Electronics, vol. 4, no. 2, pp. 626–637, June 2016.

[16] M. L. Orozco-Gutierrez, G. Spagnuolo, J. M. Ramirez-Scarpetta, G. Petrone, and C. A. Ramos-Paja, “Optimized configuration of mismatched photovoltaic arrays,” IEEE Journal of Photovoltaics, vol. 6, no. 5, pp. 1210–1220, Sept. 2016.

[17] Q. Li and P. Wolfs, “A review of the single phase photovoltaic module integrated converter topologies with three different dc link configurations,” IEEE Transactions on Power Electronics, vol. 23, no. 3, pp. 1320–1333, May 2008.

[18] Y. Zhou, L. Liu, and H. Li, “A high-performance photovoltaic module-integrated converter (mic) based on cascaded quasi-z-source inverters (qzsi) using egan fets,” IEEE Transactions on Power Electronics, vol. 28, no. 6, pp. 2727–2738, June 2013.

[19] S. Maity and P. K. Sahu, “Modeling and analysis of a fast and robust module-integrated analog photovoltaic mpp tracker,” IEEE Transactions on Power Electronics, vol. 31, no. 1, pp. 280–291, Jan. 2016.

[20] G. R. Walker and P. C. Sernia, “Cascaded dc-dc converter connection of photovoltaic modules,” IEEE Trans. Power Electron., vol. 19, no. 4, pp. 1130–1139, July 2004.

[21] R. Kadri, J. P. Gaubert, and G. Champenois, “Nondissipative string current diverter for solving the cascaded dc-dc converter connection problem in photovoltaic power generation system,” IEEE Transactions on Power Electronics, vol. 27, no. 3, pp. 1249–1258, Mar. 2012.

[22] S. M. Chen, T. J. Liang, and K. R. Hu, “Design, analysis, and implementation of solar power optimizer for dc distribution system,” IEEE Transactions on Power Electronics, vol. 28, no. 4, pp. 1764–1772, Apr. 2013.

[23] A. J. Hanson, C. A. Deline, S. M. MacAlpine, J. T. Stauth, and C. R. Sullivan, “Partial-shading assessment of photovoltaic installations via module-level monitoring,” IEEE Journal of Photovoltaics, vol. 4, no. 6, pp. 1618–1624, Nov. 2014.

[24] T. Shimizu, M. Hirakata, T. Kamezawa, and H. Watanabe, “Generation control circuit for photovoltaic modules,” IEEE Transactions on Power Electronics, vol. 16, no. 3, pp. 293–300, May 2001.

[25] P. S. Shenoy, K. A. Kim, B. B. Johnson, and P. T. Krein, “Differential power processing for increased energy production and reliability of photovoltaic systems,” IEEE Trans. Power Electron., vol. 28, no. 6, pp. 2968–2979, 2013.

[26] C. Olalla, D. Clement, M. Rodriguez, and D. Maksimovic, “Architectures and control of submodule integrated dc-dc converters for photovoltaic applications,” IEEE Trans. Power Electron., vol. 28, no. 6, pp. 2980–2997, 2013.

[27] Y. Levron, D. Clement, B. Choi, C. Olalla, and D. Maksimovic, “Control of submodule integrated converters in the isolated-port differential power-processing photovoltaic architecture,” IEEE J. Emerging Selected Topics Power Electron., vol. 2, no. 4, pp. 821–832, Dec. 2014.

[28] C. Olalla, C. Deline, D. Clement, Y. Levron, M. Rodriguez, and D. Maksimovic, “Performance of power-limited differential power processing architectures in mismatched pv systems,” IEEE Trans. Power Electron., vol. 30, no. 2, pp. 618–631, Feb. 2015.

[29] S. Qin, S. T. Cady, A. D. Dominguez-Garcia, R. C. N. Pilawa-Podgurski, “A Distributed Approach to Maximum Power Point Tracking for Photovoltaic Submodule Differential Power Processing,” IEEE Trans. Power Electron., vol. 30, no. 4, pp. 2024-2040, April 2015.

[30] A. Diab-Marzouk and O. Trescases, “Sic-based bidirectional cuk converter with differential power processing and mppt for a solar powered aircraft,” IEEE Transactions on Transportation Electrification, vol. 1, no. 4, pp. 369–381, Dec. 2015.

[31] R. Bell and R. C. N. Pilawa-Podgurski, “Decoupled and distributed maximum power point tracking of series-connected photovoltaic submodules using differential power processing,” IEEE Journal of Emerging and Selected Topics in Power Electronics, vol. 3, no. 4, pp. 881–891, Dec. 2015.

[32] M. S. Zaman, Y. Wen, R. Fernandes, B. Buter, T. Doorn, M. Dijkstra, H. J. Bergveld, and O. Trescases, "A cell-level differential power processing ic for concentrating-pv systems with bidirectional hysteretic current-mode control and closed-loop frequency regulation," IEEE Transactions on Power Electronics, vol. 30, no. 12, pp. 7230–7244, Dec. 2015.

[33] S. Qin, C. B. Barth, and R. C. N. Pilawa-Podgurski, "Enhancing microinverter energy capture with submodule differential power processing," IEEE Transactions on Power Electronics, vol. 31, no. 5, pp. 3575–3585, May 2016.

[34] Y. T. Jeon, H. Lee, K. A. Kim, and J. H. Park, "Least power point tracking method for photovoltaic differential power processing systems," IEEE Transactions on Power Electronics, vol. 32, no. 3, pp. 1941–1951, Mar. 2017.

[35] M. G. Villalva, J. R. Gazoli, and E. Filho, "Comprehensive approach to modeling and simulation of photovoltaic arrays," IEEE Trans. Power Electron., vol. 24, no. 5, pp. 1198–1208, May 2009.

[36] K. A. Kim, C. Xu, J. Lei, and P. T. Krein, "Dynamic photovoltaic model incorporating capacitive and reverse-bias characteristics," IEEE J. Photovoltaics, vol. 3, no. 14, pp. 1334–1341, 2013.

[37] D. Jena and V. V. Ramana, "Modeling of photovoltaic system for uniform and non-uniform irradiance: A critical review," Renewable and Sustainable Energy Reviews, vol. 52, pp. 400–417, 2015.

[38] H. Zhou, J. Zhao, and Y. Han, "Pv balancers: Concept, architectures, and realization," IEEE Trans. Power Electron., vol. 30, no. 7, pp. 3479–3487, July 2015